

# Identification of Regulators of the Three-Dimensional Polycomb Organization by a Microscopy-Based Genome-wide RNAi Screen

Inma Gonzalez,<sup>1,2</sup> Julio Mateos-Langerak,<sup>1,2</sup> Aubin Thomas,<sup>1</sup> Thierry Cheutin,<sup>1</sup> and Giacomo Cavalli<sup>1,\*</sup>

<sup>1</sup>Institute of Human Genetics, UPR1142 CNRS, 141 Rue de la Cardonille, 34396 Montpellier Cedex 5, France

<sup>2</sup>These authors contributed equally to this work

\*Correspondence: [giacomo.cavalli@igh.cnrs.fr](mailto:giacomo.cavalli@igh.cnrs.fr)

<http://dx.doi.org/10.1016/j.molcel.2014.03.004>

## SUMMARY

Polycomb group (PcG) proteins dynamically define cellular identities through epigenetic repression of key developmental genes. PcG target gene repression can be stabilized through the interaction in the nucleus at PcG foci. Here, we report the results of a high-resolution microscopy genome-wide RNAi screen that identifies 129 genes that regulate the nuclear organization of Pc foci. Candidate genes include PcG components and chromatin factors, as well as many protein-modifying enzymes, including components of the SUMOylation pathway. In the absence of SUMO, Pc foci coagulate into larger aggregates. Conversely, loss of function of the SUMO peptidase Velo disperses Pc foci. Moreover, SUMO and Velo colocalize with PcG proteins at PREs, and Pc SUMOylation affects its chromatin targeting, suggesting that the dynamic regulation of Pc SUMOylation regulates PcG-mediated silencing by modulating the kinetics of Pc binding to chromatin as well as its ability to form Polycomb foci.

## INTRODUCTION

Polycomb group (PcG) proteins were initially identified as factors maintaining repression of homeotic (HOX) genes during development (Duncan, 1982). Later work demonstrated a more dynamic role for PcG proteins in repressing many other developmental regulators (reviewed in Schuettengruber and Cavalli, 2009; Schuettengruber et al., 2007). In *Drosophila*, PcG proteins are recruited to chromatin by specific DNA elements, called PcG response elements (PREs). Interestingly, physical contact between two PREs that can be located at Mb distances or even on different chromosomes can enhance PcG-dependent silencing (Bantignies and Cavalli, 2011; Rosa et al., 2013).

PcG proteins form three large multimeric complexes: the Pleihomeotic repressive complex (PhoRC) (Klymenko et al., 2006), the Polycomb repressive complex 1 (PRC1) (Shao et al., 1999), and the Polycomb repressive complex 2 (PRC2) (Czermin et al., 2002). Additional PcG-containing complexes, which

contribute to the diverse functions of PcG proteins, have also been purified, suggesting that the composition of the known PcG complexes might be dependent upon tissue and developmental stage. Furthermore, there are PcG factors that are not stable components of known PcG complexes; therefore, they could not be identified by biochemical purification of the PcG complexes (Grimaud et al., 2006). These proteins might interact transiently with PcG complexes or might be part of yet-to-be-identified PcG complexes (Otte and Kwaks, 2003).

PcG proteins were originally identified by genetic screenings in *Drosophila* through the observation of body plan transformations (so-called PcG phenotypes) due to misexpression of homeotic (HOX) genes. This early genetic evidence led to an estimated number of 30–40 PcG genes in *Drosophila* (Jürgens, 1985), far below the number of PcG genes known today, suggesting that several PcG-related genes might have escaped genetic screening and subsequent biochemical studies.

Pc localizes in the nucleus at foci (also called Pc bodies), and their dynamic organization and intensity distribution changes during development (Cheutin and Cavalli, 2012). PcG target genes located at considerable linear distances along a chromosome can cluster within Pc foci (Bantignies et al., 2011; Sexton et al., 2012), and PcG-mediated silencing of homeotic genes is stabilized by long-distance interactions of HOX gene clusters (Bantignies et al., 2011).

In addition to long-range interactions of PcG target genes, many other contacts involve distant chromatin regions (Bantignies and Cavalli, 2011; Hou et al., 2012; Sexton et al., 2012; Tolhuis et al., 2011). This suggests that nuclear components may regulate 3D genome architecture. Here, we present a genome-wide RNAi screen to identify factors involved in the regulation of the 3D distribution of PcG proteins.

## RESULTS

### Primary RNAi Screen for Genes that Regulate the Nuclear Organization of Polycomb

Immunofluorescence (IF) and imaging of Pc-GFP fusion constructs show that Pc localizes in the nucleus in foci, which have no apparent distribution preferences besides a clear exclusion from pericentromeric heterochromatin (Figure 2B). To look for molecular factors involved in PcG function, we performed an RNAi screen in *Drosophila* S2 cells, looking for changes in the Pc-IF pattern by high-resolution confocal

microscopy (e.g., a loss of Pc staining, diffuse Pc staining, sharper Pc foci, etc.). Although the Pc distribution in S2 cells was characteristic, there was significant cell-to-cell variability. Therefore, large numbers of cells were studied for each gene knockdown. As a counterstain for the image analysis, as well as to assist in the interpretation of the specificity of the results, we simultaneously labeled DNA with DAPI. The screening procedure is summarized in [Figure S1A](#), available online.

We screened two RNAi libraries provided by the *Drosophila* RNAi Screening Center (DRSC; [www.flyrnai.org](http://www.flyrnai.org)) ([Ramadan et al., 2007](#)); the first, a genome-wide library, was analyzed in duplicate, and the second, a transcription factor library, was analyzed in triplicate. The genome-wide library contains, in 66 384-well plates, more than 24,000 unique dsRNAs targeting 13,900 genes covering practically the entire fly gene compendium. The transcription factor library contains, in nine 384-well plates, 1,890 unique dsRNAs targeting 993 known transcription-related proteins, such as DNA binding and nuclear proteins. In addition to these two libraries, we custom prepared two plates containing multiple replicas of dsRNAs targeting known PcG-related factors. These control plates were transfected and subsequently analyzed under the same conditions ([Figures S1B–S1E](#)).

S2 cells were transfected with both RNAi libraries ([Figure S1](#)). Pc was knocked down (KD) as a positive control in the genome-wide screen. As further controls, we knocked down *Pc*, *Su(z)12*, *Sce*, and *Su(var)205*, since KD affected Pc nuclear distribution during preliminary studies (data not shown). As negative controls we used dsRNA against either GFP or LacZ. Stained plates were imaged using a high-content screening spinning disk confocal microscope equipped with a 60×/NA1.2 water immersion objective to obtain the best possible resolution in high-throughput mode. As a result of imaging all the plates, we obtained 1.5 million two-channel images. These images were automatically treated and analyzed (see [Supplemental Experimental Procedures](#)) to extract and characterize, in an unbiased way, the list of genes whose downregulation had modified the Pc staining pattern ([Figures 1, 2, S2, and S3](#)).

### Secondary Validation Screen

In order to minimize the rate of false positives, we performed a secondary screen with a selection of candidate genes from the primary screen. We chose genes clustering with known PcG-related genes, and we selected (when available at the DRSC) additional validation dsRNAs that were not present in the genome-wide library. This resulted in a list of 214 candidate genes and 288 dsRNAs, plus 96 controls.

The custom RNAi library was screened in quintuplicate following similar labeling, imaging, and image analysis procedures as used for the primary screen. Seventy-five genes were confirmed as positive by this subsequent analysis (which gives a total of 129 positives when added to the 54 hits from the transcription factor screen; see [Table S1](#)). As expected, the majority of genes that were not confirmed were those classified as weak positives in the primary genome-wide screen.

To further characterize the phenotypes, we devised an automated selection of the most representative cells for each gene, dsRNA, or well (see companion website: <http://flyepigenome.igh.cnrs.fr/PCscreen>) and clustered their phenotypes in two

ways. First, we clustered hierarchically all the phenotypes produced by each dsRNA. This method produced a full, detailed, and continuous classification tree ([Figures S2 and S3A](#)). As a second method, we used k-means clustering and found that the data could be robustly classified into four clusters ([Figure 2](#)). The first cluster was comprised mainly of Pc itself, with KD resulting in an obvious loss of Pc staining. KD of genes in the second cluster produced more intense Pc foci. KD of genes in the third cluster produced a loss of Pc foci and the appearance of more diffuse nuclear staining. The final cluster, similar to cluster three, was characterized by a phenotype of weaker intensity of Pc foci; this phenotype was clearly defined by computer analysis but barely detectable upon visual inspection, emphasizing the high sensitivity of the automated image analysis. In rare cases, different dsRNAs targeting the same gene produced slightly different phenotypes and, as a consequence, some genes were placed in two different clusters.

Analysis of the gene functions indicated that the most enriched ontologies were presumably related to PcG function and to chromatin organization ([Figure 1A](#)). Among these, PcG proteins themselves came out in clusters 3 and 4, as expected ([Franke et al., 1995](#)). The brahma and cohesin complexes appeared particularly enriched among the positives. Moreover, 23 positive genes were not or were poorly characterized, and among them, some contained protein-protein or protein-DNA interaction domains, including chromo-, bromo-, and AT-rich interaction domains, in addition to catalytic regions, such as peptidase, phosphatase, and kinase domains. These genes constitute an interesting set of candidates for future studies.

### Components of the SUMOylation Pathway Affect the Organization of Polycomb Foci in *Drosophila*

One of the most prominent phenotypes found in our screen was produced by KD of *smt3*, which encodes the *Drosophila* small ubiquitin-related modifier (SUMO) protein ([Huang et al., 1998](#)). SUMO is covalently bound to other proteins and plays important roles in regulating their activity, stability, protein-protein interactions, and cellular localization. SUMOs are conjugated to target proteins through a cascade of reactions that typically involve three enzymes: an activating enzyme, E1, a conjugating E2 enzyme, and usually a SUMO ligase (E3), which increases the efficiency of SUMO conjugation. Before being conjugated to its targets, SUMO has to undergo maturation by cleavage of a short C-terminal extension from the precursor by a processing protease. SUMO modification can be reversed by SENPs (SUMO/sentrin-specific peptidases) ([Ulrich, 2009](#)).

In our screen, KD of SUMO (*smt3*) caused redistribution of Pc to fewer and more intense Pc foci ([Figure 2D](#)). Among the other positives, we found *Su(var)2-10*, a PIAS protein linked to SUMOylation ([Hari et al., 2001](#)), and *veloren (velo)* ([Berdnik et al., 2012](#)), a gene that encodes a polypeptide containing a putative cysteine-type SUMO peptidase domain ([Li and Hochstrasser, 2000](#)). The human homologs of *velo*, SENP6 and SENP7, have SUMO-deconjugating activity ([Lima and Reverter, 2008](#)). Consistent with a function opposed to SUMO conjugation, KD of *velo* produced a strong phenotype, namely diffuse staining of Pc, the opposite phenotype to that observed after KD of *smt3* ([Figure 2E](#)).

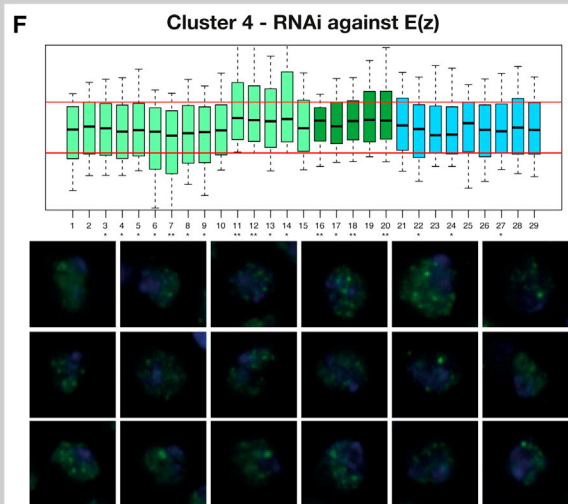
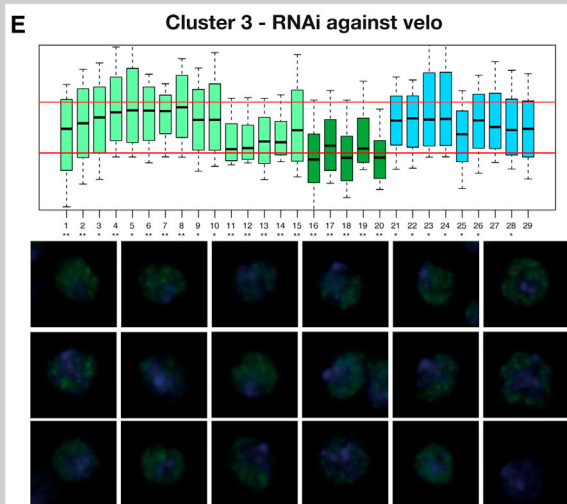
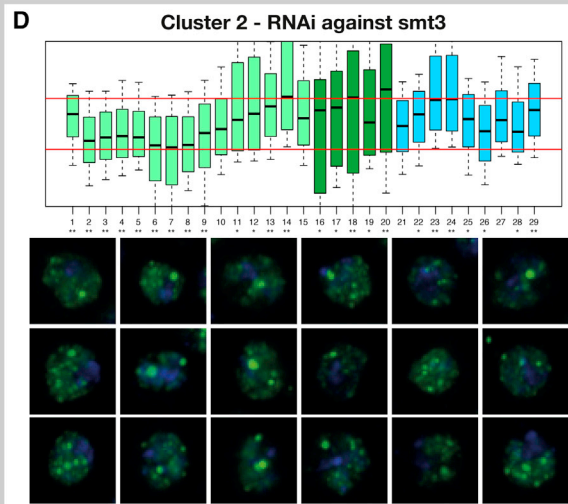
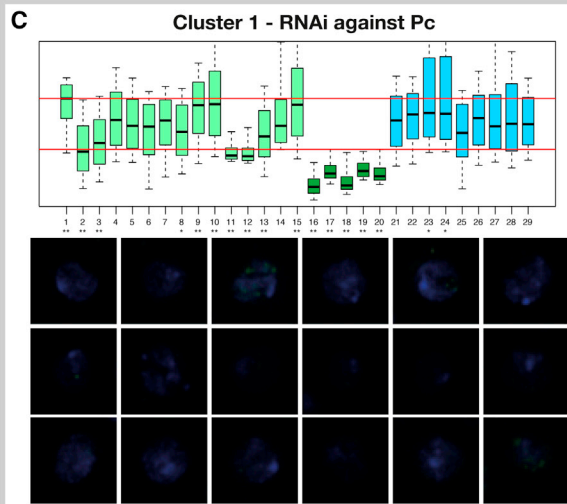
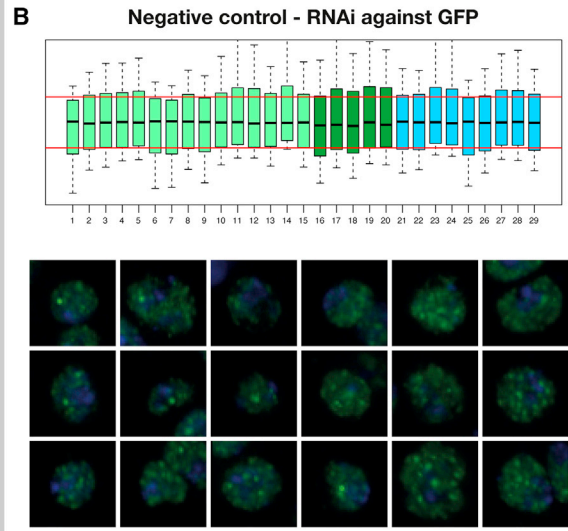


**A** **Cluster 1**  
Kap-alpha3, Pc

**Cluster 2**  
Bap60, brm, Cap, CG9775, CG9839, gw, mor, Pp4-19C, SMC1, smt3, Snr1

**Cluster 3**  
akirin, alphaCop, Arc-p20, ari-1, Axn, baf, bys, Caf1, Cenp-C, CG10321, CG10426, CG13773, CG14641, CG1832, CG2577, CG32271, CG34422, CG3523, CG4266, CG6370, CG7056, Chd3, chinmo, Ckllalpha, Cp1, cype, Dek, E(bx), east, Edc3, Egfr, Fs(2)Ket, gzfz, Hcf, HLH106, Hsc70-3, ial, Iswi, l(2)not, mip130, mip40, msl-1, msl-2, Mtor, Nedd8, Nup153, pea, ph-d, pip, Roc1a, Sce, sec13, Sfrmbt, Smd3, tlk, trx, ush, velo, Vha44

**Cluster 4**  
Act79B, AGO1, Ald, AP-2, Arc-p20, Arp66B, ball, Bap170, BRWD3, bys, C15, Cap, Cenp-C, CG15141, CG17181, CG17186, CG1908, CG4936, CG5708, CG6370, CG7154, CG8216, CG9775, CG9890, chif, croi, CycT, dalao, drk, Dsor1, e(y)3, E(z), Edc3, eIF-2gamma, Su(var)3-9, Fer1, flfl, gig, gw, Hel25E, HmgD, Kap-alpha3, kay, l(3)mbt, Lmpt, luna, MED19, Mes2, nerfin-1, Nipped-B, pho, Poxn, Pp4-19C, PPP4R2r, Rpb11, RunxB, SA, sbb, SC35, Sin3A, SMC1, Smd3, sr, stg, Su(var)2-10, Su(var)205, Su(z)12, Taf6, trr, ush



(legend on next page)

We expressed hairpin constructs to KD either *smt3* or *velo* using tissue-specific drivers. The KD efficiency was verified by immunostaining experiments using anti-SUMO and anti-Velo antibodies (Figures S4J–S4O). Depletion of SUMO in the wing pouch of wing imaginal discs, using the nubbin GAL4 driver, induced a Pc redistribution similar to cultured cells (compare Figures 3E–3H' with Figure 3D), whereas no effect was detected on the staining of the control, RNA polymerase II (Figures S4D–S4I). Since Pc is targeted to chromatin through the interaction of its chromodomain with the trimethylated lysine 27 of histone H3 (H3K27me3), we stained SUMO-depleted wing discs for H3K27me3. Importantly, the large Pc foci observed after depletion of SUMO frequently colocalize with H3K27me3 foci (Figures 3M–3P), suggesting their association with chromatin.

To KD *velo* in the posterior compartment of imaginal discs, we used the engrailed GAL4 line. Similarly to *velo* KD cultured cells (Figure 2E), there was a more diffuse Pc staining pattern (Figures 3A–3D') in the posterior compartment (KD) compared to the anterior (WT). Immunostaining of RNA polymerase II (data not shown) and H3K27me3 (Figures S4A–S4C) was not affected, suggesting that the effects of *velo* KD are specific for PRC1. We then costained Pc and Polyhomeotic (Ph), another core component of PRC1. Ph colocalized with Pc in *smt3* (Figures 3F and 3F') and *velo* (Figures 3B and 3B') KDs, suggesting that, in both cases, the relocalization affects the whole PRC1 complex.

### Pc Is SUMOylated Both In Vivo and In Vitro

The human Polycomb protein, Pc2, is SUMOylated and is itself a SUMO E3 ligase (Kagey et al., 2003) that SUMOylates other chromatin-associated factors including CTCF (MacPherson et al., 2009), Dnmt3a (Li et al., 2007), or Bmi1 (Ismail et al., 2012). However, SUMOylation of Pc in *Drosophila* has not been studied. Recombinant GST-Pc purified from bacteria produced a slower-migrating band in an in vitro SUMO conjugation reaction, which was not detected in the absence of ATP (Figure 4A), indicating that Pc can be covalently bound to SUMO in vitro.

Next, we investigated whether Pc is a target for SUMOylation in vivo. Only a small fraction of most SUMO substrates are SUMOylated at any given time. This is due to the high rate of enzymatic cleavage of the SUMO-protein isopeptide bond by SUMO proteases or isopeptidases (Hay, 2005). To increase the

proportion of SUMOylated endogenous substrate, S2 cells were transfected with FLAG-SUMO. Anti-FLAG immunoprecipitates from nuclear extracts were analyzed by western blotting (WB) with anti-Pc, revealing a slower-migrating band corresponding to SUMOylated Pc not detected in controls (Figure 4B). The 20 kDa shift of this band is consistent with the binding of a single SUMO molecule. Moreover, we detected significantly lower levels of SUMOylated Pc in the absence of the SUMO protease inhibitor, iodoacetamide (IAA) (Figure 4B). When anti-Pc (instead of anti-FLAG) was used to immunoprecipitate from SUMO-transfected cells, we detected two bands; a lower band corresponding to unmodified Pc and a higher molecular weight band corresponding to the SUMOylated form of Pc (Figure 4C).

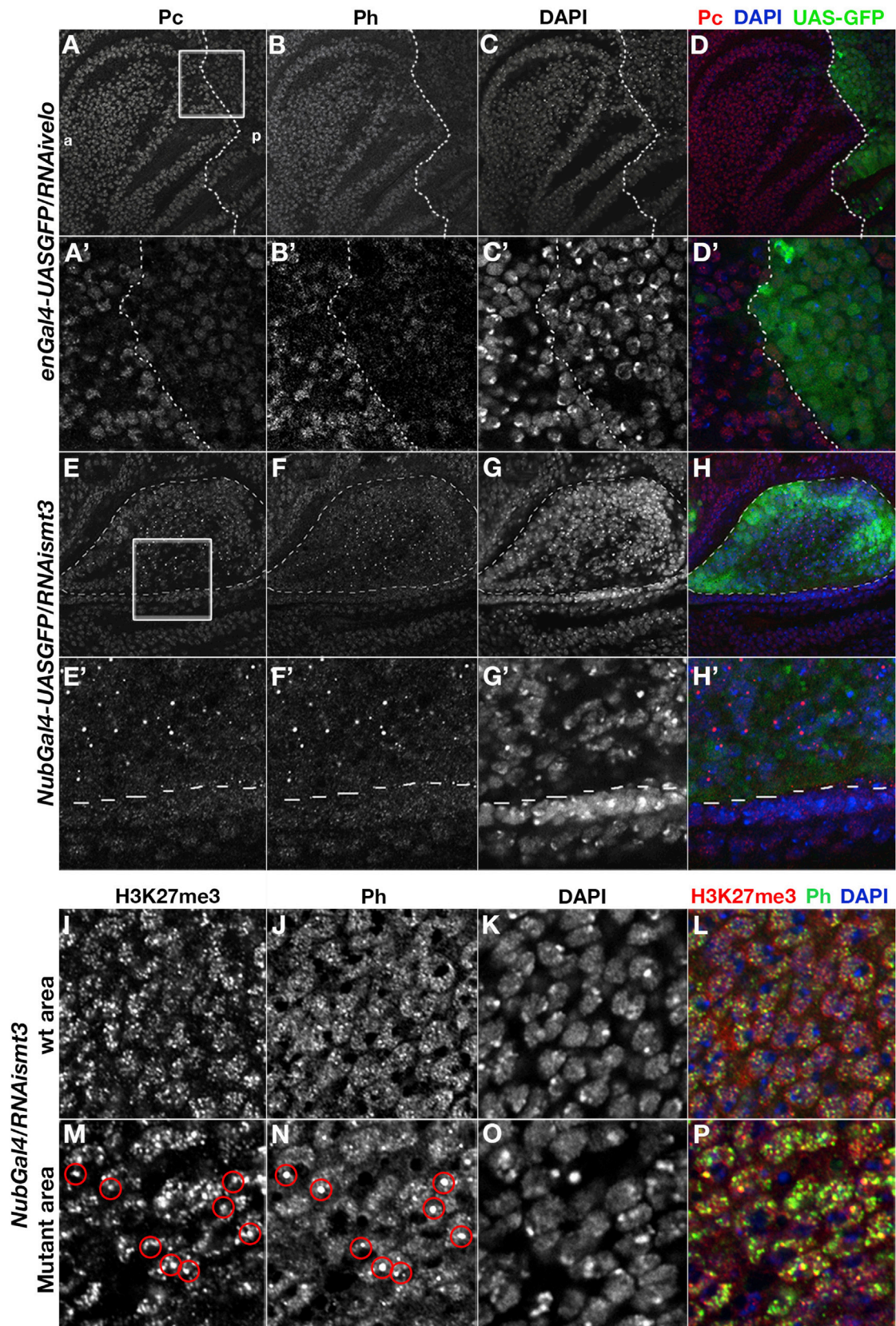
Analysis of Pc sequence using the computational prediction program SUMOsp 2.0 (<http://sumosp.biocuckoo.org/>) revealed three SUMO conjugation consensus motifs at lysine residues 128, 145, and 268 (Figure S5A). We substituted K128, K145, and K268 with arginine residues (R) using site-directed mutagenesis. Coexpression of the wild-type, or Pc mutant proteins together with SUMO and Ubc9 in S2 cells, followed by IP with anti-Pc and WB using anti-HA and anti-SUMO, showed that wild-type Pc and all single mutants were efficiently conjugated (data not shown). In contrast, the triple mutant FLAG-HA-Pc-KR3 demonstrated strongly reduced SUMOylation levels (Figure 4D). This suggests that the tested lysine residues are potential SUMOylation target sites in vivo. The observed residual SUMOylation levels of the Pc-KR3 mutant could be explained by the fact that the Pc protein sequence contains 32 additional lysine residues, four of which reside in low-probability nonconsensus SUMO attachment sites, which may be SUMOylated when the protein is mutated. In summary, these experiments show that *Drosophila* Pc can be conjugated by SUMO in vivo on, at least, three different lysine residues.

### Velo Is a SUMO Peptidase that De-SUMOylates Pc

To study a possible role for Velo in the deconjugation of SUMO-conjugated substrates, we performed an in vivo de-SUMOylation assay to observe the spectrum of proteins conjugated with SUMO upon *velo* overexpression or KD in S2 cells (Figure 4F). Western blot analysis using anti-SUMO of wild-type cell lysates showed a specific pattern of proteins conjugated with SUMO, in addition to free SUMO. KD of *smt3* globally reduced the levels of all SUMOylated substrates, as well as the

### Figure 2. Clusters and Representative Images of Selected Genes

Candidate genes are classified in four discrete clusters by k-means. (A) For each cluster we show the list of genes contained and data distributions and representative cells from one negative control well (B) as well as one example of one gene KD for each cluster (C–F). For each KD, boxplots show the distribution of 29 cell-based parameters reflecting, in light green, the texture of Pc-IF; in dark green, the intensities of Pc-IF; and, in blue, the parameters reflecting changes in DAPI staining as follows: (1) Pc-IF Texture Information Measures of Correlation 1, (2) Pc-IF Texture Information Measures of Correlation 2, (3) Pc-IF Texture Correlation, (4) Pc-IF Texture Variance, (5) Pc-IF Texture Sum Variance, (6) Pc-IF Texture Sum Entropy, (7) Pc-IF Texture Entropy, (8) Pc-IF Texture Sum Average, (9) Pc-IF Texture Difference Entropy, (10) Pc-IF Texture Contrast, (11) Pc-IF Texture Gabor X, (12) Pc-IF Texture Gabor Y, (13) Pc-IF Texture Inverse Difference Moment, (14) Pc-IF Texture Angular Second Moment, (15) Pc-IF Texture Difference Variance, (16) Pc-IF Mean Intensity, (17) Pc-IF Integrated Intensity, (18) Pc-IF St.Dev. of the Intensity, (19) Pc-IF Minimum Intensity, (20) Pc-IF Maximum Intensity, (21) DAPI Texture Correlation, (22) DAPI Mass Displacement, (23) DAPI Texture Gabor Y, (24) DAPI Texture Gabor X, (25) DAPI Texture Information Measures of Correlation 1, (26) DAPI Texture Information Measures of Correlation 2, (27) DAPI Texture Contrast, (28) DAPI Texture Sum Average, (29) DAPI Pc-IF Correlation. Boxplots represent the median, 25% and 75% percentiles (whiskers 10% and 90%) of the distribution of each parameter. The red lines represent the position of the 25% and 75% percentiles of the negative controls. Asterisks mark highly significant differences ( $p < 0.01$ ) in one (\*) or two (\*\*) of the replicas for every parameter. Eighteen representative cells are shown for each example. Images are cut out of the sample full-field images shown in Figure S3B. DAPI staining is in blue, and Pc-IF is in green. Images were normalized by the intensities for the corresponding negative controls. Images are  $11 \times 11 \mu\text{m}$ . See also Figure S3.



(legend on next page)

free SUMO (Figure 4F). Most importantly, KD of *velo* changes the equilibrium between SUMO-conjugated proteins and free SUMO, resulting in an increase in the amount of SUMOylated proteins and a decrease in the levels of free SUMO. In contrast, *Velo* overexpression induced a strong decrease in the global levels of SUMOylated proteins and an increase in free SUMO when compared with the control.

Furthermore, cotransfection with *Velo* led to a significant reduction in the levels of SUMO-conjugated Pc (Figure 4E, line 2). To test whether *Velo* requires its catalytic domain to de-SUMOylate Pc, we repeated the *in vivo* de-SUMOylation assay after cotransfecting cells with *Velo*CS, a mutant (C502S) that disrupts the catalytic domain. We did not observe changes in the level of SUMOylated-Pc compared to the control conditions (Figure 4E, line 3), indicating that the catalytic domain is necessary for the de-SUMOylation of Pc. In summary, these experiments show that *Velo* is a SUMO peptidase that can de-SUMOylate Pc.

### SUMO Conjugation of Pc Directly Modifies Nuclear Organization of Polycomb Foci

To address if the lack of SUMOylation is directly responsible for the observed redistribution of Pc in *smt3* KD cells, we expressed in S2 cells either the triple mutant fused to GFP (Pc-KR3:GFP), a constitutively SUMOylated Pc protein by fusing SUMO to the C terminus of Polycomb (Kang et al., 2010; Nayak et al., 2009; Ross et al., 2002), or the wild-type Pc tagged with GFP (Pc:GFP), which shows a similar nuclear distribution compared to endogenous Pc. Pc-KR3:GFP formed larger Pc foci when compared to Pc:GFP, similar to those found after KD of *smt3* (Figure 4G). In contrast, Pc-SUMO:GFP showed a diffuse distribution compared to Pc:GFP, similar to those found after KD of *velo* (Figure 4G). An unbiased quantification of the distribution of the different GFP-fused versions of Pc among cells with similar

expression levels confirmed these observations (Figure S5D). Therefore, SUMOylation of Pc regulates the nuclear distribution of Pc directly.

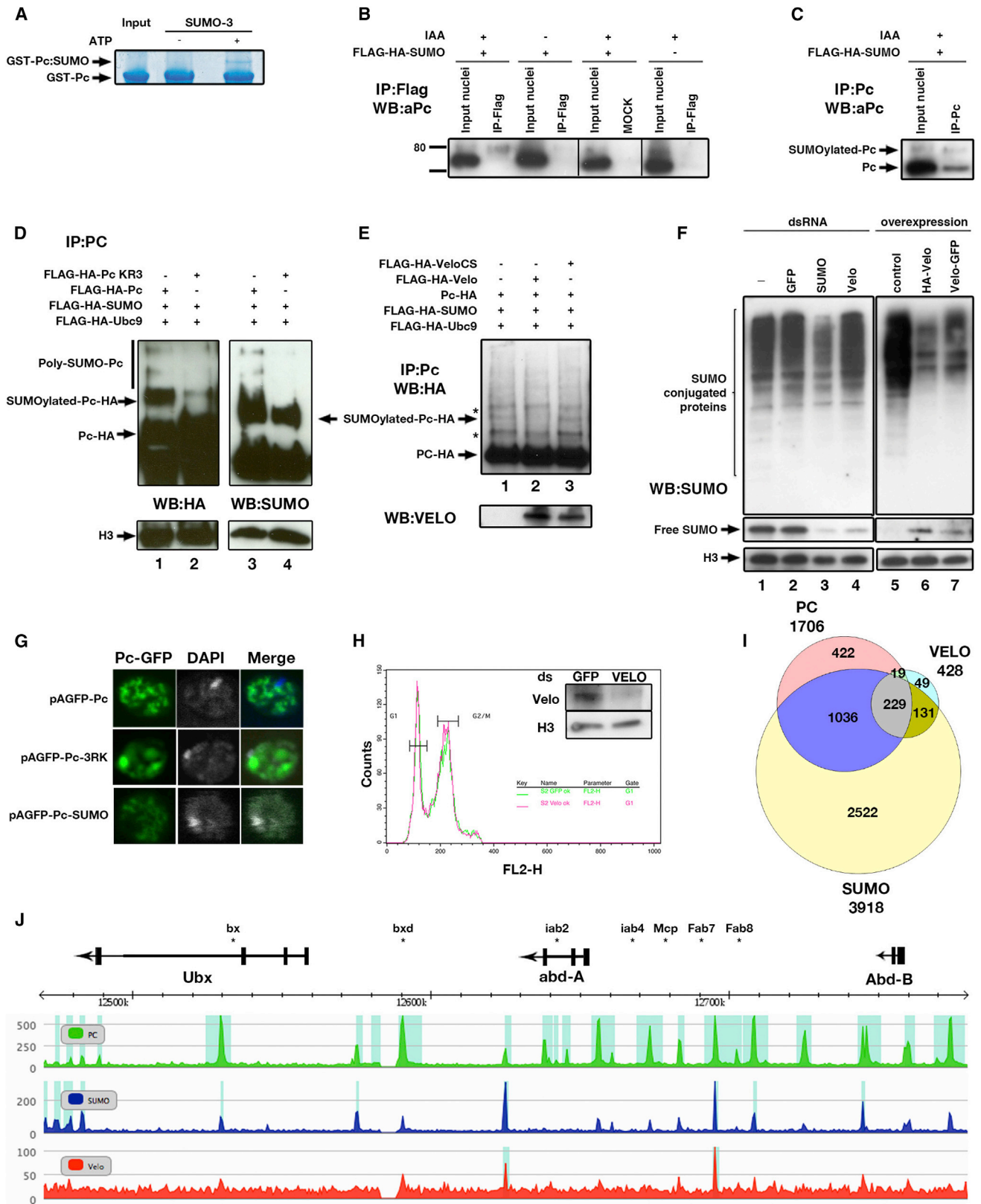
### Velo and SUMO Bind to Chromatin and Colocalize with Pc

In order to analyze whether *Velo* and SUMO exert their function on chromatin, we raised antibodies against the two *Drosophila* proteins (see Supplemental Experimental Procedures). Cellular fractionation experiments (Figure S5B) revealed a 100 kDa band corresponding to *Velo* in the cytoplasm and the nucleus, with most of the nuclear protein fraction associated with chromatin.

We then performed ChIP experiments followed by high-throughput DNA sequencing (ChIP-seq) in S2 cells. Comparison of the Pc binding profile with previously published Polycomb response elements (PREs) in S2 cells (Schwartz et al., 2010) showed a strong overlap (86% of Polycomb sites from Schwartz et al. are bound by Pc). Strikingly, both SUMO and *Velo* frequently colocalized with Pc at known Pc-binding sites (Figure 4J). Most Pc binding sites are associated with SUMO and most *Velo* sites are bound by Pc (Figure 4I), implicating a prominent fraction of the chromatin associated with the SUMO machinery in Pc-related functions. Furthermore, the vast majority of *Velo* binding sites (84.3%) are occupied by SUMO, showing that these proteins act in concert at chromatin. Whereas most Pc binding sites are also bound by SUMO, a significant number of SUMO binding sites are not associated with Pc. Most of these sites correspond to active promoter regions that are also bound by RNA Pol II and H3K4me3 (Figure S5C), in agreement with SUMO 1 and SUMO 2 distribution in human cells (Neyret-Kahn et al., 2013). Despite the strong overlap of Pc, *Velo*, and SUMO chromatin binding profiles, double immunostaining experiments of *Drosophila* imaginal discs of *Velo* or *Sumo* in conjunction with *Ph* revealed only a

**Figure 3. Distribution of Polycomb in Wing Imaginal Discs after Knockdown of *velo* and *smt3***

- (A) Immunostaining of Pc.  
 (A') Magnification of (A). "a" indicates the anterior compartment containing wild-type cells. "p" indicates the posterior compartment where enGAL4 drives the expression of the RNAi transgene for *velo*. A clear decrease of the intensity of Pc foci is observed in this compartment after KD of *velo*.  
 (B) Immunostaining of Ph.  
 (B') Magnification of (B).  
 (C) Labeling with DAPI.  
 (C') Magnification of (C).  
 (D) Merge of (A), (C), and GFP (in green) marking the expression domain of the enGAL4 line.  
 (D') Magnification of (D).  
 (E) Immunostaining of Pc.  
 (E') Magnification of (E). An increase of the size of some Pc foci is observed in the pouch where nubGAL4 drives the expression of the RNAi transgene for *smt3*.  
 (F) Immunostaining of Ph.  
 (F') Magnification of (F).  
 (G) Labeling with DAPI.  
 (G') Magnification of (G).  
 (H) Merge of (E), (G), and GFP (in green) marking the expression domain of the NubGAL4 line.  
 (H') Magnification of (H).  
 (I) Immunostaining with H3K27me3 in the wild-type region of wing imaginal discs.  
 (J) Immunostaining with Ph.  
 (K) Labeling with DAPI.  
 (L) Merge of (I), (J), and (K).  
 (M) Immunostaining with H3K27me3 in the region of KD *smt3* of wing imaginal disc.  
 (N) Immunostaining with Ph.  
 (O) Labeling with DAPI.  
 (P) Merge of (M), (N), and (O). See also Figure S4.



(legend on next page)

partial colocalization of Velo and SUMO with Pc foci (Figures S5E–S5G and Figures S5H–S5J), suggesting that Pc foci mainly contain Pc in a hypo-SUMOylated state in vivo.

### Pc SUMOylation Levels Affect Its Chromatin Binding Affinity and Residence Time

Of note, even if the human homolog of Velo, SENP6, modulates the cell cycle (Mukhopadhyay et al., 2010), FACS analysis of cells depleted for Velo did not reveal a significant cell-cycle difference (Figure 4H), indicating that the nuclear redistribution of PcG proteins is not due to changes in cell-cycle regulation. Since it was previously reported that SUMOylation can interfere with the recruitment of transcription factors to chromatin (Chalkiadaki and Talianidis, 2005), we then tested whether the changes in the nuclear distribution of Pc upon perturbation of its SUMOylation levels might reflect impaired recruitment of PcG proteins to their target sites.

Overall Pc levels did not change after KD of components belonging to the SUMOylation pathway (Figures S6K and S6L). However, the staining of polytene chromosomes in salivary glands depleted of Velo showed a significant decrease in the number and intensity of binding sites for the PRC1 components Pc and Ph (Figures 5A–5H). We further noted that Velo depletion altered the structure of the polytene chromosomes, leading to chromosome decondensation (Figures 5E–5H); however, the localization and binding levels of polymerase II on polytene chromosomes were unchanged after KD of *velo* (Figures S6E–S6H), indicating that loss of *velo* function specifically affects binding of PcG proteins. In contrast to the effect of Velo depletion, the levels and number of binding sites for PcG proteins were not significantly affected after KD of *smt3* (Figures 5I–5L), suggesting that SUMO modification of Pc is not required for chromatin targeting in this tissue.

To extend these observations to diploid tissues, we performed ChIP assays using anti-Pc in imaginal wing discs depleted of Velo or SUMO. The occupancy of Pc on known PREs significantly decreased in wing imaginal discs depleted of Velo (Figures 5M, 5O, and S6I). By contrast, we did not observe any significant changes in Pc binding, or in the levels of H3 and H3K27me3 at the same PREs after KD of *smt3* (Figures 5N, 5P, and S6J).

In order to test whether the binding kinetics of Pc to chromatin was affected upon KD of *velo* and *smt3*, we performed fluorescence recovery after photobleaching (FRAP) microscopy to compare the recovery of PC-GFP in wing imaginal disc nuclei after KD of *velo* and *smt3*. Interestingly, KD of *smt3* strongly slows down the recovery of PC-GFP, indicating that Pc binds more stably to chromatin. In contrast, the recovery of PC-GFP is much faster in nuclei KD for *velo* (Figure 5Q). These results demonstrate that SUMOylation strongly affects the kinetics of Pc binding to chromatin.

### Velo Mutant Flies Show Homeotic Transformations Similar to PcG Mutants

To understand the relationship between the in vivo biological roles of *velo* and PcG function, we examined the effect of *velo* loss of function during fly development. Velo depletion at the embryonic stage using a NanosGal4 driver induced segmentation defects that were detected in preparations of late embryonic cuticles, with disruption or loss of denticle belts and frequent denticle fusions (Figures 6A and 6B). These phenotypes resemble those described for PcG mutants, reflecting a PcG-dependent control of segmentation genes (McKeon et al., 1994). Interestingly, similar cuticular phenotypes have been described in a *smt3* KD (Smith et al., 2011).

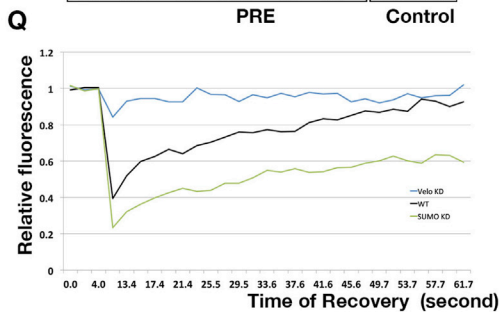
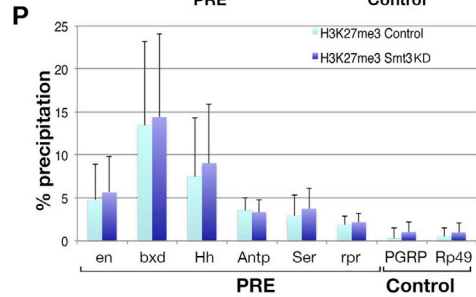
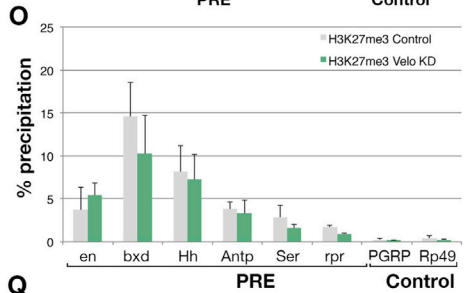
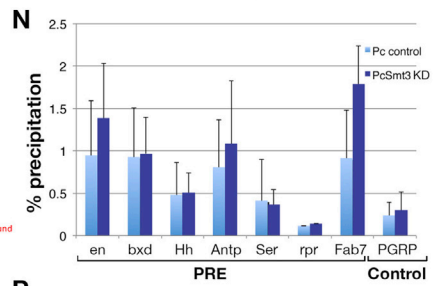
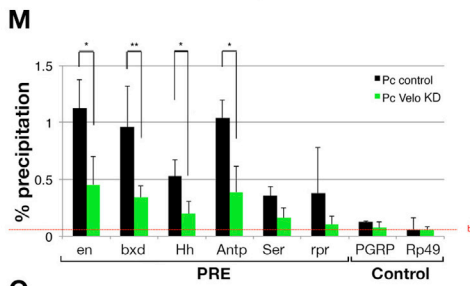
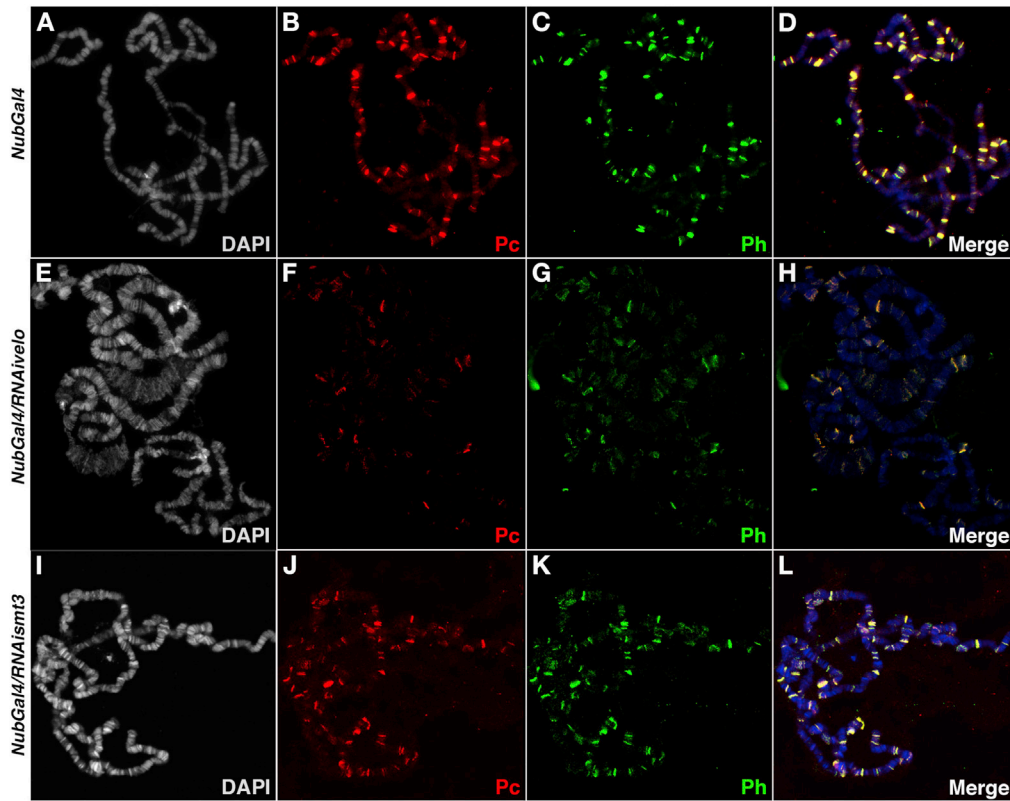
We next analyzed wing imaginal discs depleted of Velo using the enGal4 driver. We observed derepression of the homeotic gene *Ultrabithorax* (*Ubx*) in cells in the posterior compartment, in which the *velo* gene is downregulated (Figures 6C and 6D). This phenotype is similar to that of Pc mutants (Cabrera et al., 1985). When KD of *velo* was performed at a later developmental stage (using a NubGal4 driver), mutants displayed smaller wings and halteres compared with the wild-type, consistent with derepression of *Ubx* and consequent partial transformation of wings to halteres (Figures 6E–6G).

## DISCUSSION

In this study, we combined two high-resolution imaging-based screens in order to discover factors involved in the 3D arrangement of Pc in the *Drosophila* nucleus. We identified, in an

### Figure 4. Smt3 and Velo Regulate the SUMOylation State of Polycomb and Colocalize with Polycomb at Polycomb Response Elements

(A) Modification of *Drosophila* Pc using SUMO-3 Conjugation kit. Proteins were separated by 4%–20% SDS-PAGE and visualized with Coomassie blue stain. (B and C) Immunoprecipitation analysis of SUMOylated Pc. S2 cells were transiently transfected with FLAG-tagged *Smt3*, and cell lysates were either immunoprecipitated with anti-FLAG (B) or anti-Pc (C). Western blots were analyzed with anti-Pc. The positions of Pc and its SUMOylated forms are indicated. (D) SUMOylation of Pc lysine mutants in vivo. S2 cells expressing FLAG-HA-tagged Pc or Pc-KR3 mutants (Pc K128R, K145R, and K268R) were immunoprecipitated using anti-Pc and analyzed by western blotting with anti-HA (lanes 1 and 2) or with anti-SUMO (lanes 3 and 4). (E) Velo is a SUMO peptidase that requires a catalytically intact protease domain to specifically desumoylate Pc. S2 cells were transfected with the indicated plasmids. Immunoprecipitation was performed with anti-Pc (IP) from transfected cell lysates, and western blot was detected with anti-HA. Asterisks indicate nonspecific bands. Overexpression levels of Velo were controlled by western blotting using anti-Velo antibodies. (F) The SUMO peptidase Velo regulates the equilibrium of SUMO-conjugated proteins and free SUMO. S2 cells were either not transfected (lane 1) or transfected with GFP dsRNA (lane 2), *smt3* dsRNA (lane 3), *velo* dsRNA (lane 4), DNA empty vector (lane 5), HA-Velo (lane 6), or Velo-GFP (lane 7). SUMOylated proteins were detected by western blotting using anti-SUMO. H3 is shown a loading control. (G) Subcellular localization of GFP-Pc and GFP-Pc-KR3 or a constitutively SUMOylated form of Pc (GFP-Pc-SUMO). S2 cells were transfected with the indicated GFP-tagged Pc expression constructs and visualized by live-cell confocal fluorescence microscopy. (H) Cell-cycle profile of S2 cells comparing control cells (dsGFP) and cells depleted for *velo* (dsVelo). (I) Venn diagrams showing overlap between bound regions of indicated proteins. (J) Genomic distribution of PC, SUMO, and VELO in the Bithorax complex (BXC) of chromosome 3R determined by ChIP-seq analysis. Significantly enriched regions are indicated by blue shadowed boxes (see Experimental Procedures for details). Asterisks indicate known PREs. The ChIP-Seq data can be browsed at our paper companion website (<http://flyepigenome.igh.cnrs.fr/PCscreen>) and are available in GEO under the accession number GSE55303. See also Figure S5.



(legend on next page)

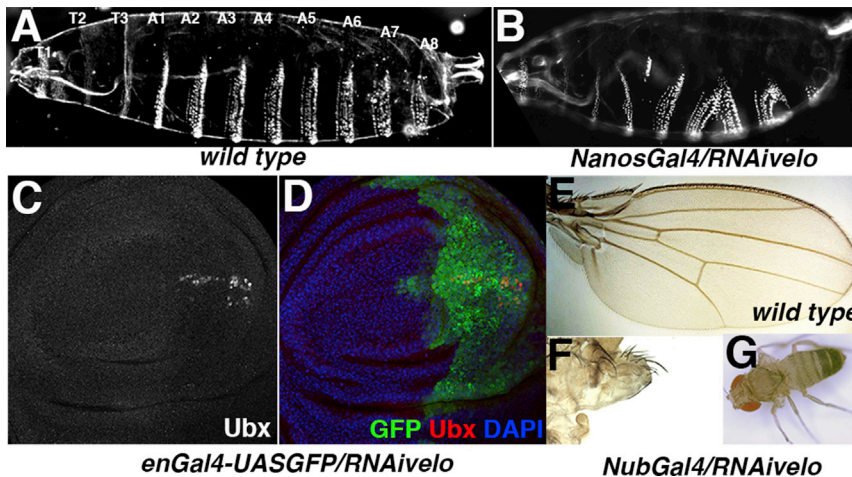


**Figure 6. In Vivo Analysis of Loss of Function of *velo* during *Drosophila* Development**

(A) Wild-type larval cuticle showing the pattern of denticle belts.  
 (B) Larval cuticles of embryos depleted of *velo* (*NanosGal4/RNAi velo*). KD of *velo* mutant embryos displays disruption and fusion of denticle belts. The cuticles do not show homeotic phenotypes.  
 (C) Immunostaining analysis using anti-Ubx on wing imaginal discs where *Velo* is depleted in the posterior compartment (*enGal4-UASGFP/RNAi velo*). Derepression of *Ubx* is detected in a subset of cells in the posterior compartment.  
 (D) Merge of the different immunostainings of *Ubx* (red), DAPI (blue), and GFP (green), which marks the expression area of *enGal4*.  
 (E) Wing from a wild-type fly.  
 (F) Wing from *Nub-Gal4/UAS-RNAi velo* showing a reduction and partial transformation of the wing. Images are to scale.  
 (G) Adult fly *Nub-Gal4/UAS-RNAi velo*.

unbiased way, more than 100 genes, and characterized two of them, showing that the SUMO peptidase *Velo* is required for Pc targeting to chromatin and that a tightly regulated balance of Pc SUMOylation levels is required for the 3D organization of Pc foci and the function of PcG proteins.

#### High-Resolution Microscopy RNAi Screen Identifies Regulators of the Nuclear Organization of Pc Foci

The identification of all PcG proteins can be traced back to genetic screens, which had a decisive role in gene discovery. However, genetic screens also have limitations; it is difficult to identify genes with substantial maternal components in screens based on embryonic phenotypes; adult screens based on heterozygous mutations are affected by the fact that many genes display haplo-sufficiency; and induced mutations demonstrate irregular coverage of the genome. Moreover, mutations resulting in pleiotropic effects might interfere with the normal development of the organism, thereby preventing the display of the phenotypes of interest.

With the present screen, we identified two major classes of modifiers. The first class contained genes whose KD effects

were not restricted to Pc distribution but also induced changes in the DAPI staining pattern, most likely reflecting large-scale chromatin rearrangement. The second class (followed up in this study) contained genes specifically affecting Pc distribution, with little or no effect on general chromatin organization as revealed by DAPI staining.

The current screen detected all positive controls, and no negative controls were classified as hits, indicating that the assay is robust and efficient. Six core PcG genes out of the eleven known to date were detected, including members of the PhoRC, PRC2, and PRC1 complexes. The members that were not identified are characterized by having redundant function with another PcG protein (*Pho1* for the PhoRC complex, *Esc* and *Esc1* for the PRC2 complex, and *Psc* and *Su(z)2* for the PRC1 complex), suggesting that, as for many other screening procedures, redundancy hampers detection in RNAi-based screens.

Many of the hits were chromatin components, and several of them have been recently related to PcG proteins. The genes coding for cohesins and the cohesion associated proteins, *Smc1*, *Smc3/Cap*, and *Sa* were pulled down in a biotinylation tagging strategy (Strübbe et al., 2011). Another example is *Hcf*,

#### Figure 5. *Velo* Plays a Crucial Role in Chromatin Recruitment of Polycomb

(A–L) Immunostaining of polytene chromosomes.

(A–D) Staining of control *UAS-Dcr2*; *nubGal4* chromosomes. (A) Labeled with DAPI. (B) Staining with anti-Pc. (C) Staining with anti-Ph. (D) Merge of (A), (B), and (C).

(E–H) Same staining scheme as above of *UAS-Dcr2*; *nubGal4-UASGFP/UAS-RNAi velo* chromosomes.

(I–L) Same staining scheme as above of *UAS-Dcr2*; *nubGal4-UASGFP/UAS-RNAi smt3* chromosomes.

(M) qChIP analysis using anti-Pc antibodies of *MS1096Gal4/UAS-RNAiGFP* wing imaginal discs (control, black bars) and *MS1096Gal4/UAS-RNAi velo* wing imaginal discs (*velo* KD, green bars). ChIP signal levels are represented as percentage of input chromatin. Values represent means  $\pm$  SD from four to six independent experiments. \* $p < 0.05$ , \*\* $p < 0.01$ , unpaired, two-tailed Student's *t* test.

(N) qChIP analysis using Pc antibodies of *MS1096Gal4/UAS-RNAiGFP* wing imaginal discs (control, light blue bars) and *MS1096Gal4/UAS-RNAi smt3* wing imaginal discs (*smt3* KD, dark blue bars). Error bars represent SD.

(O) qChIP analysis using H3K27me3 antibodies of *MS1096Gal4/UAS-RNAiGFP* wing imaginal discs (control, gray bars) and *MS1096Gal4/UAS-RNAi velo* wing imaginal discs (*velo* KD, green bars). Error bars represent SD.

(P) qChIP analysis using H3K27me3 antibodies of *MS1096Gal4/UAS-RNAiGFP* wing imaginal discs (control, light blue bars) and *MS1096Gal4/UAS-RNAi smt3* wing imaginal discs (*smt3* KD, dark blue bars). Error bars represent SD.

(Q) FRAP experiments monitoring the recovery of fluorescence of PC-GFP in wild-type imaginal disc (black line), upon KD of *smt3* (green line) and upon KD *velo* (blue line). FRAP experiments were performed on wing imaginal disc expressing PC-GFP by collecting 2D images every 2 s for 2 min. Student's *t* test comparing the recovery of PC-GFP after 20 s: WT versus KD of *smt3* ( $p < 0.01$ ); WT versus KD of *velo* ( $p < 0.001$ ). See also Figure S6.

a factor involved in both PcG and trxG functions (Rodriguez-Jato et al., 2011). Other modifying factors are members of the trithorax group (trxG) of genes, which counteract PcG function during the regulation of Hox and other developmental genes. Among these, *trx*, *trr*, and *E(bx)* are prominent, as they are linked to the deposition and recognition of the histone mark H3K4me<sub>3</sub>, which counteracts H3K27me<sub>3</sub>. Other prominent trxG genes identified in the screen encode for multiple subunits of the brahma complex (*brm*, *Bap60*, *Bap170*, *mor*, and *Snr1*).

Components of the dosage compensation machinery and nucleoporins were also identified in the screen. Since these factors are involved in the formation of active chromatin domains (Mendjan et al., 2006; Vaquerizas et al., 2010), they may compete for PcG binding in a similar way to trxG components. However, the possibility of indirect effects cannot be excluded at this point. In particular, other nuclear import proteins were also scored as positive (Kap- $\alpha$ 3, Sec13); and another possible explanation for some of these hits is that impaired nuclear transport of Pc or other PcG components may affect the integrity of Pc foci.

Other hits are either uncharacterized genes or were not previously related to PcG function. An interesting class among these contains proteins with sequence-specific DNA binding activity (C15, Chinmo, Crol, Fer1, HLH106, Kay, Lmpt, Luna, Poxn, RunxB, and Ush), or proteins linked to sequence-specific repression of transcription, such as Mip130 and Mip40, two components of the repressive MMB complex that contains Myb (Georlette et al., 2007; Korenjak et al., 2004). This is an intriguing finding, since previous attempts to predict the sequence-specific code for PcG targeting had limited success (Schuettengruber and Cavalli, 2009; Schuettengruber et al., 2009). An attractive possibility is that multiple transcription factors may contribute to PcG recruitment at subsets of their target genes (Okulski et al., 2011).

Other interesting Pc foci modifiers include factors involved in RNA binding and metabolism (Ago1, Dek, Hel25E, Pea, SmD3), and in signaling pathways (Axn) often linked to posttranslational protein modification (for example, kinases, including Dsor1, Ial, Stg, and Tik; phosphatases, including, Pp'-19C, PPP4R2r; ubiquitylation factors, such as Gw, Roc1; and proteins involved in SUMOylation, such as Su(var)2-10, Velo, and Smt3). These genes may open new avenues for PcG regulation mediated by posttranslational modification of Pc or of its partners.

### Role of SUMOylation in Pc Recruitment to Chromatin and Nuclear Architecture

SUMO is implicated in a plethora of cellular events (reviewed in Hay, 2005). Increasing evidence suggests that SUMO may also contribute to protein solubility (Marblestone et al., 2006; Panavas et al., 2009). At a molecular level, SUMOylation affects protein function by creating and abolishing binding interfaces, or by inducing conformational changes that result in altered interactions (for detailed examples, see Johnson, 2004).

SUMOylation of human Pc2 increases its binding affinity for H3K27me<sub>3</sub> (Kang et al., 2010). In *C. elegans*, SUMOylation of SOP-2, a SAM-domain protein with homology to *Drosophila* Scm and Ph, is thought to induce SOP-2 localization into Pc foci and to repress the expression of Hox genes (Zhang et al., 2004). In *Drosophila*, SUMOylation of the PRC1-interacting pro-

tein, Scm (Sex Comb on Midleg), reduces its association with chromatin (Smith et al., 2011). Sfbmt, a subunit of the PhoRC complex, has been identified in a screen for factors involved in SUMO-dependent transcriptional repression (Stielow et al., 2008). Comparison of genes identified in this screen with ours revealed only a limited overlap of seven genes: *Sfbmt*, *kay*, *Su(var)2-10*, *sbb*, *Chd3*, and *CG7056*. The fact that the screen paradigms are largely different might explain why Pc was not previously linked to SUMO by Stielow et al. and emphasizes the importance of performing screens based on independent readouts.

A well-characterized example of the importance of SUMO in the regulation of nuclear architecture is the formation of promyelocytic leukemia protein (PML) nuclear bodies (reviewed by Seeler and Dejean, 2003). In PML bodies, a combination of SUMO and SIMs (SUMO interaction motifs) enables the interaction of many proteins to nucleate and establish a PML nuclear body scaffold (Shen et al., 2006). As another example, the SENP7 SUMO peptidase was shown to maintain HP1 on pericentric heterochromatin, whereas its depletion does not affect H3K9me<sub>3</sub> levels (Maison et al., 2012). In *Drosophila*, SUMOylation affects the formation of insulator bodies. Both the suppression and the induction of SUMOylation reduce the coalescence of insulator proteins (Capelson and Corces, 2006; Golovnin et al., 2012). This situation differs from the case of Pc, showing that SUMO can affect different nuclear proteins in specific ways that depend on how it affects protein-protein interactions in multiprotein complexes.

How does SUMOylation affect the nuclear organization of Pc? One possibility is that the effect of SUMO may be specifically linked to the nuclear organization of Pc foci. Depletion of the SUMO peptidase, Velo, induced loss of PcG targeting in diploid cells and in polytene chromosomes (Figure 5). On the other hand, SUMO depletion did not perturb Pc targeting, although it did cause marked coalescence of PcG proteins to form massive Pc foci. We have shown through FRAP experiments in a well-characterized in vivo system (Cheutin and Cavalli, 2012) that Pc suffers from significant changes in its residence time in Pc-foci as a consequence of *smt3* or *velo* KD (Figure 5Q). The data thus suggest a scenario for the role of SUMO in the nuclear organization of Pc. Without SUMO, more stable Pc may promote protein-protein interactions with other PRC1 complexes and generate the formation of stable nuclear aggregates that are observed upon *smt3* KD. A limited degree of SUMOylation may prevent the coalescence of PRC1 complexes within the nucleus, whereas excess SUMO may solubilize Pc away from its target chromatin.

SUMO modification has been shown to promote protein solubility (Sabate et al., 2012), and this property prevents aggregation of  $\alpha$ -synuclein, an aggregation-prone protein implicated in Parkinson's disease (Krumova et al., 2011). Our data suggest that SUMOylation may similarly promote the solubility of PRC1 in vivo, thereby preventing aggregation of PRC1 in the nucleus. Low, physiologic levels of Pc SUMOylation may act as "fluidifier" of PRC1-mediated chromatin interactions, preventing excessive in vivo aggregation at Pc foci while allowing robust chromatin targeting and efficient silencing of its target genes. Future studies should test whether other PcG or trxG components are

SUMOylated, and to what extent the interplay of these modifications regulates PcG and trxG function in different cell types and during development.

In summary, we presented here a screening approach that is highly reproducible and sensitive, and relies on a cell biology assay that is completely independent from previous screens. Recently, a screen based on DNA FISH has allowed factors involved in chromosome pairing to be identified (Joyce et al., 2012). These approaches have the potential to be extended to many other biological processes occurring within or beyond the cell nucleus.

## EXPERIMENTAL PROCEDURES

### Screen Image Acquisition and Analysis

Plates were imaged in an Opera (Perkin Elmer) spinning-disk confocal microscope equipped with a 60x/NA 1.2 and providing a lateral resolution of 0.25  $\mu\text{m}$ . Images corresponding to three Z optical sections were maximum intensity projected along the z axis into a single image using ImageJ (U.S. National Institutes of Health, <http://imagej.nih.gov/ij/>). The rest of the image analysis procedure was performed using CellProfiler (Carpenter et al., 2006) (Broad Institute Imaging Platform, MIT/Harvard, <http://www.cellprofiler.com>). Images were analyzed at the Orchestra computer cluster of Harvard Medical School, and the resulting measurements were exported as CSV tables. Representative images for the genes selected as positives after the secondary screen can be consulted at the website <http://flyepigenome.igh.cnrs.fr/PCscreen>.

### Statistical Procedures

Data analysis was performed using the R software package (R Foundation for Statistical Computing, <http://www.R-project.org>). We normalized all the data in the genome-wide and Transcription Factors screens using the B-score (Brideau et al., 2003). Secondary screen data were normalized using the Normalized Percentage Inhibition method. Clustering was performed using the gplots package in R. Euclidean n dimensional distance was computed in combination with ward clustering.

### Gene Ontology Terms Enrichment

Gene Ontology term enrichments were calculated using DAVID 6.7 (<http://david.abcc.ncifcrf.gov>) (Huang et al., 2009). We introduced the list of positive candidate genes from either the genome-wide screen and from the transcription factors screen and used, respectively, the whole *Drosophila* genome or the list of genes present in the transcriptions factors library as background references.

### Chromatin Immunoprecipitation

ChIP on wing imaginal discs was done as described in Schuettengruber et al. (2009) with modifications as described in the [Supplemental Experimental Procedures](#).

Further details on the screening procedure, as well as information on plasmids, primer sequences, antibodies, and other experimental procedures, are provided in the [Supplemental Information](#).

## ACCESSION NUMBERS

The GEO accession number for the ChIP-Seq data reported in this paper is GSE55303.

## SUPPLEMENTAL INFORMATION

Supplemental Information includes six figures, one table, and Supplemental Experimental Procedures and can be found with this article at <http://dx.doi.org/10.1016/j.molcel.2014.03.004>.

## ACKNOWLEDGMENTS

We are thankful to the DRSC for providing the RNAi libraries, the technical means, and the expertise necessary to fulfill this study. We thank Bernd Schuettengruber and Tom Sexton for critically reading the manuscript. We thank the MRI-IGH imaging facility for critical guidance in microscopy analysis. The Leica SP8 microscope used in part of this work was financed by the Association pour la Recherche sur le Cancer (ARC) (EML20120904995). Research at the G.C. lab was supported by grants from the European Research Council (ERC-2008-AdG number 232947), the CNRS, the European Network of Excellence EpiGeneSys, the Agence Nationale de la Recherche, and the ARC. I.G. was supported by a fellowship from the Ministerio de Ciencia e Innovación/Fulbright and the ARC. J.M.-L. was supported by a fellowship from the ARC, and by the Fondation pour la Recherche Médicale.

Received: January 14, 2013

Revised: February 11, 2014

Accepted: February 24, 2014

Published: April 3, 2014

## REFERENCES

- Bantignies, F., and Cavalli, G. (2011). Polycomb group proteins: repression in 3D. *Trends Genet.* 27, 454–464.
- Bantignies, F., Roue, V., Comet, I., Leblanc, B., Schuettengruber, B., Bonnet, J., Tixier, V., Mas, A., and Cavalli, G. (2011). Polycomb-dependent regulatory contacts between distant Hox loci in *Drosophila*. *Cell* 144, 214–226.
- Berdnik, D., Favaloro, V., and Luo, L. (2012). The SUMO protease Verloren regulates dendrite and axon targeting in olfactory projection neurons. *J. Neurosci.* 32, 8331–8340.
- Brideau, C., Gunter, B., Pikounis, B., and Liaw, A. (2003). Improved statistical methods for hit selection in high-throughput screening. *J. Biomol. Screen* 8, 634–647.
- Cabrera, C.V., Botas, J., and Garcia-Bellido, A. (1985). Distribution of Ultrathorax proteins in mutants of *Drosophila* bithorax complex and its trans-regulatory genes. *Nature* 318, 569–571.
- Capelson, M., and Corces, V.G. (2006). SUMO conjugation attenuates the activity of the gypsy chromatin insulator. *EMBO J.* 25, 1906–1914.
- Carpenter, A.E., Jones, T.R., Lamprecht, M.R., Clarke, C., Kang, I.H., Friman, O., Guertin, D.A., Chang, J.H., Lindquist, R.A., Moffat, J., et al. (2006). CellProfiler: image analysis software for identifying and quantifying cell phenotypes. *Genome Biol.* 7, R100.
- Chalkiadaki, A., and Talianidis, I. (2005). SUMO-dependent compartmentalization in promyelocytic leukemia protein nuclear bodies prevents the access of LRH-1 to chromatin. *Mol. Cell. Biol.* 25, 5095–5105.
- Cheutin, T., and Cavalli, G. (2012). Progressive polycomb assembly on H3K27me3 compartments generates polycomb bodies with developmentally regulated motion. *PLoS Genet.* 8, e1002465.
- Czernin, B., Melfi, R., McCabe, D., Seitz, V., Imhof, A., and Pirrotta, V. (2002). *Drosophila* enhancer of Zeste/ESC complexes have a histone H3 methyltransferase activity that marks chromosomal Polycomb sites. *Cell* 111, 185–196.
- Duncan, I.M. (1982). Polycomblike: a gene that appears to be required for the normal expression of the bithorax and antennapedia gene complexes of *Drosophila melanogaster*. *Genetics* 102, 49–70.
- Franke, A., Messmer, S., and Paro, R. (1995). Mapping functional domains of the polycomb protein of *Drosophila melanogaster*. *Chromosome Res.* 3, 351–360.
- Georlette, D., Ahn, S., MacAlpine, D.M., Cheung, E., Lewis, P.W., Beall, E.L., Bell, S.P., Speed, T., Manak, J.R., and Botchan, M.R. (2007). Genomic profiling and expression studies reveal both positive and negative activities for the *Drosophila* Myb MuvB/dREAM complex in proliferating cells. *Genes Dev.* 21, 2880–2896.

- Golovnin, A., Volkov, I., and Georgiev, P. (2012). SUMO conjugation is required for the assembly of *Drosophila* Su(Hw) and Mod(mdg4) into insulator bodies that facilitate insulator complex formation. *J. Cell Sci.* **125**, 2064–2074.
- Grimaud, C., Nègre, N., and Cavalli, G. (2006). From genetics to epigenetics: the tale of Polycomb group and trithorax group genes. *Chromosome Res.* **14**, 363–375.
- Hari, K.L., Cook, K.R., and Karpen, G.H. (2001). The *Drosophila* Su(var)2-10 locus regulates chromosome structure and function and encodes a member of the PIAS protein family. *Genes Dev.* **15**, 1334–1348.
- Hay, R.T. (2005). SUMO: a history of modification. *Mol. Cell* **18**, 1–12.
- Hou, C., Li, L., Qin, Z.S., and Corces, V.G. (2012). Gene density, transcription, and insulators contribute to the partition of the *Drosophila* genome into physical domains. *Mol. Cell* **48**, 471–484.
- Huang, H.W., Tsoi, S.C., Sun, Y.H., and Li, S.S. (1998). Identification and characterization of the SMT3 cDNA and gene encoding ubiquitin-like protein from *Drosophila melanogaster*. *Biochem. Mol. Biol. Int.* **46**, 775–785.
- Huang, W., Sherman, B.T., and Lempicki, R.A. (2009). Systematic and integrative analysis of large gene lists using DAVID bioinformatics resources. *Nat. Protoc.* **4**, 44–57.
- Ismail, I.H., Gagné, J.P., Caron, M.C., McDonald, D., Xu, Z., Masson, J.Y., Poirier, G.G., and Hendzel, M.J. (2012). CBX4-mediated SUMO modification regulates BMI1 recruitment at sites of DNA damage. *Nucleic Acids Res.* **40**, 5497–5510.
- Johnson, E.S. (2004). Protein modification by SUMO. *Annu. Rev. Biochem.* **73**, 355–382.
- Joyce, E.F., Williams, B.R., Xie, T., and Wu, C.T. (2012). Identification of genes that promote or antagonize somatic homolog pairing using a high-throughput FISH-based screen. *PLoS Genet.* **8**, e1002667.
- Jürgens, G. (1985). A group of genes controlling the spatial expression of the bithorax complex in *Drosophila*. *Nature* **316**, 153–155.
- Kagey, M.H., Melhuish, T.A., and Wotton, D. (2003). The polycomb protein Pc2 is a SUMO E3. *Cell* **113**, 127–137.
- Kang, X., Qi, Y., Zuo, Y., Wang, Q., Zou, Y., Schwartz, R.J., Cheng, J., and Yeh, E.T. (2010). SUMO-specific protease 2 is essential for suppression of polycomb group protein-mediated gene silencing during embryonic development. *Mol. Cell* **38**, 191–201.
- Klymenko, T., Papp, B., Fischle, W., Köcher, T., Schelder, M., Fritsch, C., Wild, B., Wilm, M., and Müller, J. (2006). A Polycomb group protein complex with sequence-specific DNA-binding and selective methyl-lysine-binding activities. *Genes Dev.* **20**, 1110–1122.
- Korenjak, M., Taylor-Harding, B., Binné, U.K., Satterlee, J.S., Stevaux, O., Aasland, R., White-Cooper, H., Dyson, N., and Brehm, A. (2004). Native E2F/RBF complexes contain Myb-interacting proteins and repress transcription of developmentally controlled E2F target genes. *Cell* **119**, 181–193.
- Krumova, P., Meulmeester, E., Garrido, M., Tirard, M., Hsiao, H.H., Bossis, G., Urlaub, H., Zweckstetter, M., Kügler, S., Melchior, F., et al. (2011). Sumoylation inhibits alpha-synuclein aggregation and toxicity. *J. Cell Biol.* **194**, 49–60.
- Li, S.J., and Hochstrasser, M. (2000). The yeast ULP2 (SMT4) gene encodes a novel protease specific for the ubiquitin-like Smt3 protein. *Mol. Cell Biol.* **20**, 2367–2377.
- Li, B., Zhou, J., Liu, P., Hu, J., Jin, H., Shimono, Y., Takahashi, M., and Xu, G. (2007). Polycomb protein Cbx4 promotes SUMO modification of de novo DNA methyltransferase Dnmt3a. *Biochem. J.* **405**, 369–378.
- Lima, C.D., and Reverter, D. (2008). Structure of the human SENP7 catalytic domain and poly-SUMO deconjugation activities for SENP6 and SENP7. *J. Biol. Chem.* **283**, 32045–32055.
- MacPherson, M.J., Beatty, L.G., Zhou, W., Du, M., and Sadowski, P.D. (2009). The CTCF insulator protein is posttranslationally modified by SUMO. *Mol. Cell Biol.* **29**, 714–725.
- Maison, C., Romeo, K., Bailly, D., Dubarry, M., Quivy, J.P., and Almouzni, G. (2012). The SUMO protease SENP7 is a critical component to ensure HP1 enrichment at pericentric heterochromatin. *Nat. Struct. Mol. Biol.* **19**, 458–460.
- Marblestone, J.G., Edavettal, S.C., Lim, Y., Lim, P., Zuo, X., and Butt, T.R. (2006). Comparison of SUMO fusion technology with traditional gene fusion systems: enhanced expression and solubility with SUMO. *Protein Sci.* **15**, 182–189.
- McKeon, J., Slade, E., Sinclair, D.A., Cheng, N., Couling, M., and Brock, H.W. (1994). Mutations in some Polycomb group genes of *Drosophila* interfere with regulation of segmentation genes. *Mol. Genet.* **244**, 474–483.
- Mendjan, S., Taipale, M., Kind, J., Holz, H., Gebhardt, P., Schelder, M., Vermeulen, M., Buscaino, A., Duncan, K., Mueller, J., et al. (2006). Nuclear pore components are involved in the transcriptional regulation of dosage compensation in *Drosophila*. *Mol. Cell* **21**, 811–823.
- Mukhopadhyay, D., Arnaoutov, A., and Dasso, M. (2010). The SUMO protease SENP6 is essential for inner kinetochore assembly. *J. Cell Biol.* **188**, 681–692.
- Nayak, A., Glöckner-Pagel, J., Vaeth, M., Schumann, J.E., Buttman, M., Bopp, T., Schmitt, E., Serfling, E., and Berberich-Siebelt, F. (2009). Sumoylation of the transcription factor NFATc1 leads to its subnuclear relocalization and interleukin-2 repression by histone deacetylase. *J. Biol. Chem.* **284**, 10935–10946.
- Neyret-Kahn, H., Benhamed, M., Ye, T., Le Gras, S., Cossec, J.C., Lapaquette, P., Bischof, O., Ouspenskaia, M., Dasso, M., Seeler, J., et al. (2013). Sumoylation at chromatin governs coordinated repression of a transcriptional program essential for cell growth and proliferation. *Genome Res.* **23**, 1563–1579.
- Okulski, H., Druck, B., Bhalerao, S., and Ringrose, L. (2011). Quantitative analysis of polycomb response elements (PREs) at identical genomic locations distinguishes contributions of PRE sequence and genomic environment. *Epigenetics Chromatin* **4**, 4.
- Otte, A.P., and Kwaks, T.H. (2003). Gene repression by Polycomb group protein complexes: a distinct complex for every occasion? *Curr. Opin. Genet. Dev.* **13**, 448–454.
- Panavas, T., Sanders, C., and Butt, T.R. (2009). SUMO fusion technology for enhanced protein production in prokaryotic and eukaryotic expression systems. *Methods Mol. Biol.* **497**, 303–317.
- Ramadan, N., Flockhart, I., Booker, M., Perrimon, N., and Mathey-Prevet, B. (2007). Design and implementation of high-throughput RNAi screens in cultured *Drosophila* cells. *Nat. Protoc.* **2**, 2245–2264.
- Rodriguez-Jato, S., Busturia, A., and Herr, W. (2011). *Drosophila melanogaster* dHCF interacts with both PcG and TrxG epigenetic regulators. *PLoS ONE* **6**, e27479.
- Rosa, S., De Lucia, F., Mylne, J.S., Zhu, D., Ohmido, N., Pendle, A., Kato, N., Shaw, P., and Dean, C. (2013). Physical clustering of FLC alleles during Polycomb-mediated epigenetic silencing in vernalization. *Genes Dev.* **27**, 1845–1850.
- Ross, S., Best, J.L., Zon, L.I., and Gill, G. (2002). SUMO-1 modification represses Sp3 transcriptional activation and modulates its subnuclear localization. *Mol. Cell* **10**, 831–842.
- Sabate, R., Espargaro, A., Graña-Montes, R., Reverter, D., and Ventura, S. (2012). Native structure protects SUMO proteins from aggregation into amyloid fibrils. *Biomacromolecules* **13**, 1916–1926.
- Schuettengruber, B., and Cavalli, G. (2009). Recruitment of polycomb group complexes and their role in the dynamic regulation of cell fate choice. *Development* **136**, 3531–3542.
- Schuettengruber, B., Chourrout, D., Vervoort, M., Leblanc, B., and Cavalli, G. (2007). Genome regulation by polycomb and trithorax proteins. *Cell* **128**, 735–745.
- Schuettengruber, B., Ganapathi, M., Leblanc, B., Portoso, M., Jaschek, R., Tolhuis, B., van Lohuizen, M., Tanay, A., and Cavalli, G. (2009). Functional anatomy of polycomb and trithorax chromatin landscapes in *Drosophila* embryos. *PLoS Biol.* **7**, e13.
- Schwartz, Y.B., Kahn, T.G., Stenberg, P., Ohno, K., Bourgon, R., and Pirrotta, V. (2010). Alternative epigenetic chromatin states of polycomb target genes. *PLoS Genet.* **6**, e1000805.

- Seeler, J.S., and Dejean, A. (2003). Nuclear and unclear functions of SUMO. *Nat. Rev. Mol. Cell Biol.* 4, 690–699.
- Sexton, T., Yaffe, E., Kenigsberg, E., Bantignies, F., Leblanc, B., Hoichman, M., Parrinello, H., Tanay, A., and Cavalli, G. (2012). Three-dimensional folding and functional organization principles of the *Drosophila* genome. *Cell* 148, 458–472.
- Shao, Z., Raible, F., Mollaaghababa, R., Guyon, J.R., Wu, C.T., Bender, W., and Kingston, R.E. (1999). Stabilization of chromatin structure by PRC1, a Polycomb complex. *Cell* 98, 37–46.
- Shen, T.H., Lin, H.K., Scaglioni, P.P., Yung, T.M., and Pandolfi, P.P. (2006). The mechanisms of PML-nuclear body formation. *Mol. Cell* 24, 331–339.
- Smith, M., Mallin, D.R., Simon, J.A., and Courey, A.J. (2011). Small ubiquitin-like modifier (SUMO) conjugation impedes transcriptional silencing by the polycomb group repressor Sex Comb on Midleg. *J. Biol. Chem.* 286, 11391–11400.
- Stielow, B., Sapetschnig, A., Krüger, I., Kunert, N., Brehm, A., Boutros, M., and Suske, G. (2008). Identification of SUMO-dependent chromatin-associated transcriptional repression components by a genome-wide RNAi screen. *Mol. Cell* 29, 742–754.
- Strübbe, G., Popp, C., Schmidt, A., Pauli, A., Ringrose, L., Beisel, C., and Paro, R. (2011). Polycomb purification by in vivo biotinylation tagging reveals cohesin and Trithorax group proteins as interaction partners. *Proc. Natl. Acad. Sci. USA* 108, 5572–5577.
- Tolhuis, B., Blom, M., Kerkhoven, R.M., Pagie, L., Teunissen, H., Nieuwland, M., Simonis, M., de Laat, W., van Lohuizen, M., and van Steensel, B. (2011). Interactions among Polycomb domains are guided by chromosome architecture. *PLoS Genet.* 7, e1001343.
- Ulrich, H.D. (2009). SUMO protocols. Preface. *Methods Mol. Biol.* 497, v–vi.
- Vaquerizas, J.M., Suyama, R., Kind, J., Miura, K., Luscombe, N.M., and Akhtar, A. (2010). Nuclear pore proteins nup153 and megator define transcriptionally active regions in the *Drosophila* genome. *PLoS Genet.* 6, e1000846.
- Zhang, H., Smolen, G.A., Palmer, R., Christoforou, A., van den Heuvel, S., and Haber, D.A. (2004). SUMO modification is required for in vivo Hox gene regulation by the *Caenorhabditis elegans* Polycomb group protein SOP-2. *Nat. Genet.* 36, 507–511.